



## Comprehensive analysis of solar cell behavior: effects of light intensity, temperature, and operational modes

 Ersaiyn Bekbolsynov\*

Faculty of Physics and Mathematics, Bukhara State University, 11 Mukhammad Iqbol st., Bukhara, Uzbekistan

\*Correspondence: [ersaiynb@mail.ru](mailto:ersaiynb@mail.ru)

**Abstract.** This study investigates the current-voltage characteristics of a solar cell under varying light intensities, temperatures, and operational conditions to comprehensively assess its performance. The experimental approach involves measuring short-circuit current and open-circuit voltage at different light intensities and constructing current-voltage curves to analyze the solar cell's response to changing illumination levels. The dependence of open-circuit voltage and short-circuit current on temperature is also estimated to understand thermal influences on the solar cell's electrical properties. Additionally, the solar cell's behavior is examined under different operational modes, including cooling with a blower, operation without cooling, and light filtration through a glass plate. The corresponding current-voltage characteristics are plotted to evaluate the impact of thermal management and light modulation on the solar cell's efficiency and stability. Furthermore, the characteristic curve of the solar cell is determined under natural sunlight illumination to simulate real-world conditions. The findings provide valuable insights into optimizing solar cell performance for practical applications and sustainable energy systems. This research contributes to advancing our understanding of solar cell behavior under diverse environmental and operational settings, with implications for enhancing solar energy utilization and promoting renewable energy technologies. Future studies will focus on refining solar cell design and operation based on these insights to maximize efficiency and reliability in solar power generation.

**Keywords:** solar cell, current-voltage characteristics, light intensity, temperature dependence, operational modes, thermal management, renewable energy, sustainability.

### 1. Introduction

Silicon, a fundamental element in the periodic table with the atomic number 14, is widely recognized for its importance in modern technology, particularly in the semiconductor industry. Pure silicon, when isolated and characterized, displays several unique properties essential for its applications in electronics and various scientific endeavors [1]. Pure silicon primarily exists in a crystalline form with a diamond cubic crystal structure. Each silicon atom is covalently bonded to four neighboring silicon atoms, forming a stable and rigid lattice. This crystal structure contributes to silicon's robustness and resilience under varying environmental conditions [2].

One of the most notable properties of silicon is its semiconductor nature [3]. Silicon's electronic properties are influenced by its four valence electrons [4]. At absolute zero temperature, silicon behaves as an insulator due to the completely filled valence band and an empty conduction band. However, at higher temperatures or under specific conditions, silicon can become a semiconductor by promoting electrons from the valence band to the conduction band, thereby facilitating electron mobility crucial for electronic conductivity [5].

To create a  $p$  – or  $n$  – type semiconductor, pure silicon is purposefully "impurified" (doped) with triand pentavalent impurity atoms [6]. The junction formed when  $p$  – and  $n$  – type crystals are combined determines the solar cell's electrical characteristics (Figure 1). When there is no external voltage present and the system is in equilibrium, the Fermi characteristic energy level remains

constant. Electrons diffuse into the  $p$  – region and holes into the  $n$  – region due to the differences in the concentrations of electrons and holes in the two regions. A space charge-limited current area is formed by the immobile impurity atoms, and the diffusion current and the field current balance each other out in an equilibrium [7–9].

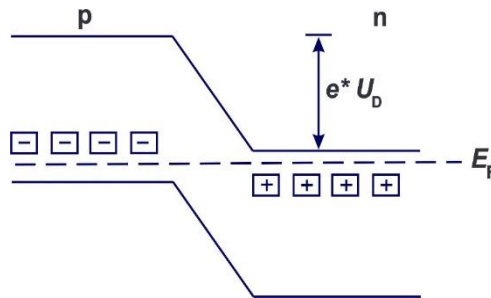


Figure 1 – The energy-band scheme’s + donors and – acceptors are located at the  $pn$  – junction, where  $e$  represents the elemental charge and  $U_D$  is the diffusion potential

The initial disparity in Fermi energy levels between the separate  $p$  – and  $n$  – regions is indicated by the diffusion potential  $U_D$  in the  $pn$  – junction, and this is contingent upon the doping level. In silicon under typical conditions, the gap between the valence and conduction bands is fixed  $E = 1.1 eV$ . The diffusion potential of silicon is between 0.5 and 0.7  $eV$ . The detail construction on Figure 2.

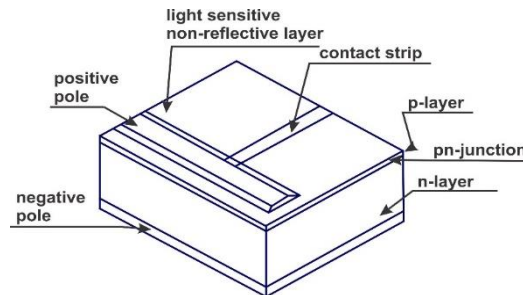


Figure 2 – Putting together a silicon solar cell

Photons from light striking the  $pn$  – junction form electron-hole pairs that are divided by the space charge [10-11]. The  $n$  – region absorbs electrons, while the  $p$  – region absorbs holes. In addition to the  $pn$  – junction, the  $p$  – layer above it also absorbs photons. The generated electrons are minority carriers in those regions because recombination significantly lowers their concentration and, consequently, their efficiency. In order for the electrons of diffusion length  $l_e$  to enter the  $n$  – layer, the  $p$  – layer needs to be thin enough:  $L_E \gg t$ , in a view of the  $t$  is the  $p$  –layer's thickness.

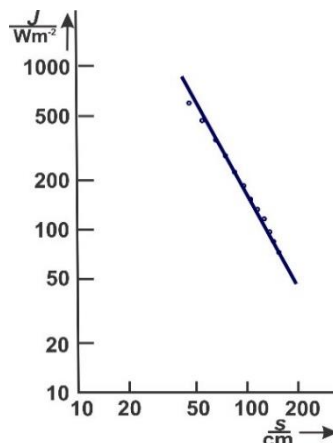


Figure 3 – Intensity of the light at standard distances from the source

When a voltage  $U$  is placed across the  $pn$  – junction and  $g$ , the number of electron-hole pairs generated per unit area, a stream of electrons and holes with a density is formed:

$$i = e * \left( e^{\frac{eU}{kT-1}} \right) * \left( \frac{n_0 D_e t}{L^2 e} + \frac{p_0 D_h}{L_h} \right) - eg \quad (1)$$

When:  $e$  – the elementary charge;  $k$  – Boltzmann's constant;  $T$  – the temperature;  $L$  – the diffusion length of electrons and holes;  $D$  – the diffusion constant for electrons and holes;  $n_0$  and  $p_0$  are equilibrium concentrations of the minority carriers.

At a constant temperature, the short-circuit current density ( $U = 0$ )  $i_s = -e * g$  is proportional to the incident light's intensity. The temperature increases with  $g$  becoming very slightly greater, less than  $10^{-2} \frac{\%}{K}$ . The voltage  $U$  is limited to reaching the same height as the diffusion potential  $U_D$ . The no-load voltage normally drops by  $-2.3 \frac{mV}{K}$  as the temperature rises because the equilibrium concentrations  $n_0$  and  $p_0$  rise with temperature:

$$n_0 \sim e^{-\frac{\Delta E}{2kT}} \quad (2)$$

This research aims to study a solar cell's current-voltage properties at various light intensities. Plot the current-voltage characteristic at various light intensities after measuring the short-circuit current and no-load voltage at various light intensities. Compared to Calculate how temperature affects the short-circuit current and no-load voltage. Additionally, we are interested in experimenting with various modes and plotting the current-voltage characteristic under various operating conditions, such as blower cooling, no cooling, and beaming light through a glass plate. The final step is to identify the characteristic curve under solar illumination.

## 2. Methods

The equipment on which the study was conducted includes a quadruple solar array, in the form of an assembly containing photovoltaic cells for generating electricity from sunlight. A device that converts thermal energy into electrical energy by utilising the Seebeck effect, namely for measuring temperature or generating electricity – a Moll-type thermopile was used as part of all equipment. The solar cell detects stray light from the benchtop reflection in addition to the light from the lamp, which is the only source of light that the thermopile measures. The distance between the light source and the solar cell can be adjusted to change the intensity of the light. Thus, the light intensity was measured using a thermopile and an amplifier at an input voltage of 10 V with equipment at different distances from the light source. To reduce the stray light, a black cloth was placed over the optical bench during the experiment. The change in distance was measured with a 1000 mm metre scale. In this case, the lamp was installed at a distance of 0.5 m from the thermopile due to the fact that the angular aperture of the latter is  $20^\circ$ . The distance between the lamp and the solar panel was more than 0.5 m, as shortening this distance may provoke distortion of the measurement results.

The main characteristics of the solar cell were measured in sunlight; that is, both direct and diffuse light were involved. Thermopile has also been used as a tool to determine the relationship between short-circuit current and light intensity, despite the fact that this equipment is only able to measure direct light due to its small angular aperture. Therefore, for comparative purposes, a black cardboard tube about 20 cm long was fixed in front of the solar cell to shield it from stray light. Thus, the thermopile and solar cell were pointed directly at the sunlight.

An electronic device used to amplify and measure various types of signals, often used in conjunction with sensors or transducers. Also used were 330 Ohm rheostats and a ceramic base designed to accommodate a standard E27 base lamp (e.g. incandescent or LED bulbs) with additional features such as a reflector, switch and protective plug. The source was an incandescent lamp (220 V/120 W) with a reflector. A powerful 1800W blower was used to control the temperature and create hot or cold air. A thermometer with an operating range of  $-10$  to  $+110$  °C was used. It is necessary to blow hot air over the solar cell and record the temperature directly in front of it with a thermometer

to accurately determine the temperature effect. It is important to note that the room temperature of the solar panels and its cells was maintained with a cold air fan. In this case, tactical contact to the cell was excluded, due to the ease of damaging its thin p-layer.

Sturdy bases, tripods, stainless steel support rods of different lengths and flexibility were used to support the entire structure. Different types of clamps were designed to hold rods or other objects at right angles, making complex operations easier. Plate holders have also been used to hold plates securely. In addition, a heavy-duty clamp was used to secure all equipment. Transparent glass panels were selected with a size of 150x100x4 mm. Glass plates were used only to observe the current-voltage relationship under different operating conditions such as fan cooling of the equipment, no cooling, and illumination through the glass plate. An electrical circuit for measuring volt-ampmetered characterisation was assembled as shown in Figure 1. Before experimental procedure the values of the no-load voltage and short-circuit current have been recorded.

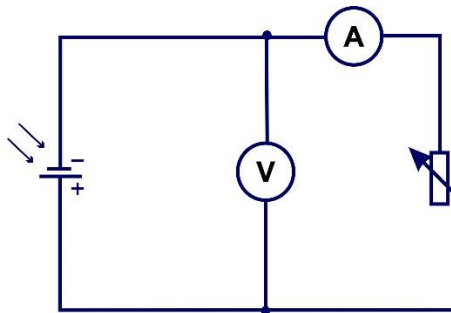


Figure 1 – Electrical circuit for measuring volt-ampmetered characterization

Two digital multimeters were used to measure voltage, current and resistance as well as other electrical parameters such as capacitance, frequency and temperature. Strong electrical cords 500 mm long and 32A amperage connect all parts of the equipment to each other.

### 3. Results and Discussion

For a more accurate and proper experiment, the short-circuit current and no-load voltage at different light intensities were first recorded. Figure 2 shows a plot of current versus voltage at different light intensities. Assume that the measuring surface receives all light that enters the 0.025 m diameter aperture. The graph illustrates a straight line on the graph representing the light intensity  $J$  dependence on distance  $s$ . One can calculate the light intensity at a distance of  $s \leq 0.5$  m by extrapolating the straight line.

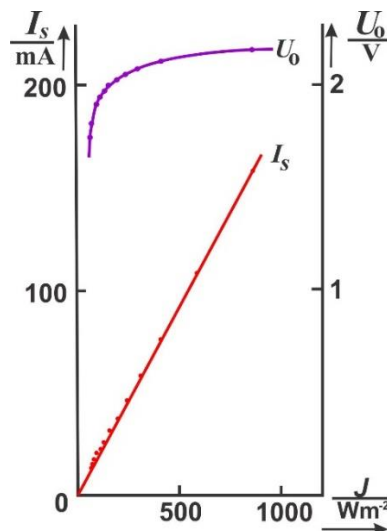


Figure 2 – The relationship between short circuit current and no-load voltage and light intensity

A solar cell with four series-connected cells that have a maximum no-load voltage of 2 V. The sensitivity of the measured equipment reached up to 0.16 mV/mW. Consequently, the intensity of light is described by the following level:

$$I_s = 1.84 * 10^{-4} \frac{A}{Wm^{-2}} * J \quad (3)$$

The values of volt-ampere characteristics were recorded at various light intensities and are displayed in Figure 3. The graph's dotted line connects the turning points of the curves, which represent the places at which the solar cell's internal resistance and the load resistor's values coincide to produce the greatest power production.

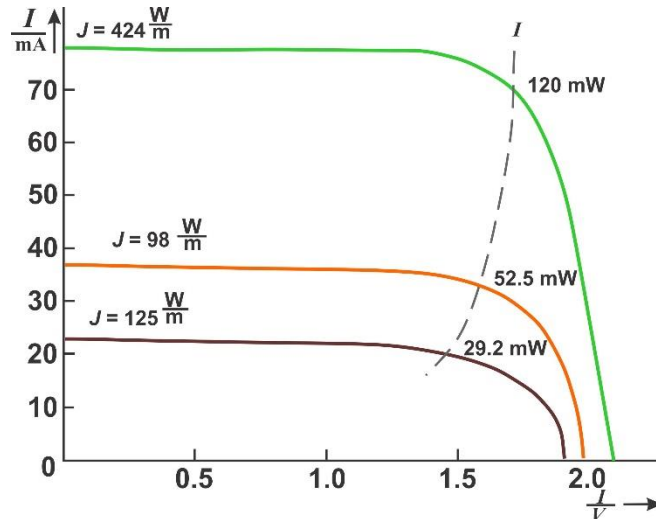


Figure 3 – Characteristics of current and voltage at various light intensities

As a result, as light intensity increases, internal resistance lowers. An efficiency of roughly 6% is obtained when the maximum output power and the incident power are compared, so solar panel area is 0.5 m<sup>2</sup>.

The research has considered the impact of temperature as well as the distribution of temperature over the hot air area. The following equality was obtained by using hot and cold air to measure the no-load voltage:

$$\frac{\Delta U_0}{\Delta T} = -8 \frac{mV}{K} \quad (4)$$

It is important to remember that the measurements can only provide a rough order of magnitude. As a result, we get a value of  $-2 \frac{mV}{K}$  for a single cell. It is impossible to quantify how the short-circuit current changes with temperature.

For completeness of the experimental data, we additionally installed a glass plate, which is able to absorb light in the infrared region and hence used to reduce the temperature rise of the solar cell. Figure 4 is a graph showing the effect of the stack effect work from different ‘modes of operation’. The graph shows three curves: the orange one refers to the fan-cooled mode; the green one indicates the fan-cooled mode; and the blue curve - when shielded with a glass plate. Note that the light intensity in the fan cooling mode is the maximum light intensity.

To identify the difference between different light sources, characteristic curves were recorded when illuminated by sunlight. Figure 5 shows a graph of the dependence of light intensity and wavelength, which shows curves from various sources. The spectral sensitivity of a silicon solar cell and the spectrum of the sun, which has a temperature of around 5800 K, and an incandescent bulb, which has a temperature of about 2000 K. Solar cells produce distinct properties when exposed to sunlight than incandescent lights do:

$$I_s = 3.04 * 10^{-4} \frac{JA}{Wm^{-2}} \quad (5)$$

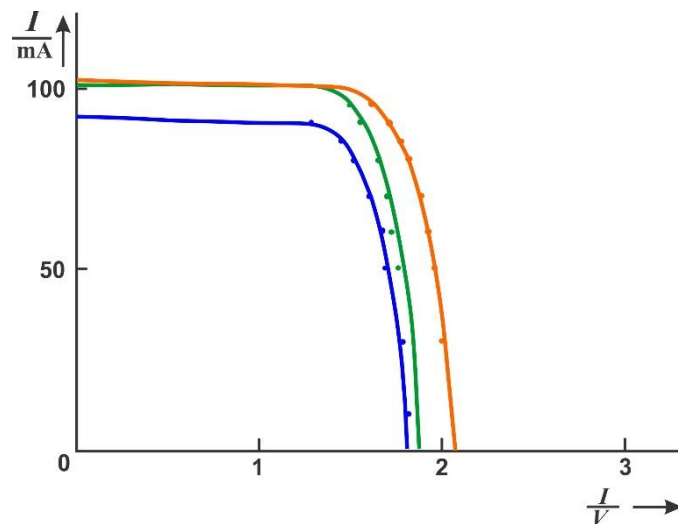


Figure 4 – Characteristics of the solar battery's current and voltage

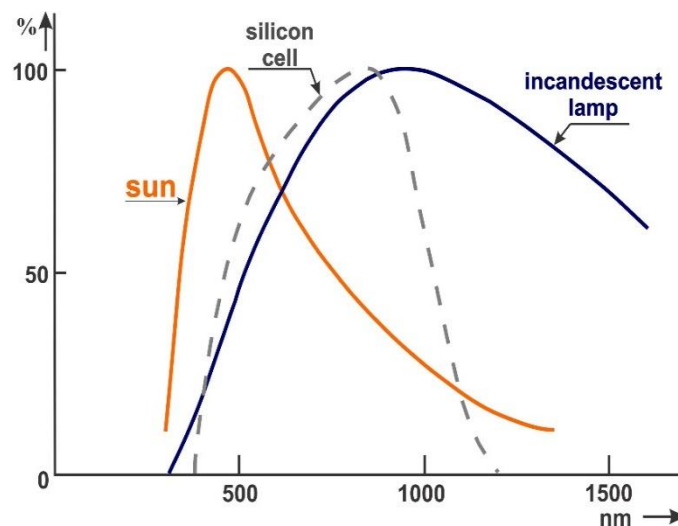


Figure 5 – Spectral characteristics of various sources

The two light sources' different spectra provide the explanation. Light from the sun produces a greater short-circuit current at the same intensity. The solar cell does not heat up as much in the infrared part of the spectrum because of this, and measurements taken with and without cooling provide identical solar properties.

#### 4. Conclusions

This investigation has provided valuable insights into the performance characteristics of a solar cell under varying light intensities, temperatures, and different operational conditions. Initially, the short-circuit current and open-circuit voltage were measured across a range of light intensities, allowing for the construction of current-voltage curves. These curves elucidated the impact of light intensity variations on the electrical output of the solar cell, crucial for understanding its efficiency under changing environmental conditions.

Subsequently, the study estimated the dependence of no-load voltage and short-circuit current on temperature. This analysis highlighted the influence of temperature fluctuations on the solar cell's electrical characteristics, offering insights into its behavior in practical applications.

Furthermore, the investigation evaluated the solar cell's performance under different operating modes, including cooling with a blower, operation without cooling, and light filtration through a glass plate. The corresponding I-V characteristics demonstrated the significance of thermal management and light modulation in optimizing the solar cell's efficiency and stability.

Moreover, the characteristic curve of the solar cell under natural sunlight illumination was determined. This final analysis provided practical data on the solar cell's behavior in real-world conditions, guiding future design and implementation strategies for solar energy systems.

In summary, the findings from this comprehensive study contribute to advancing our understanding of solar cell behavior under diverse environmental and operational settings. This knowledge is instrumental in improving the efficiency, reliability, and practicality of solar energy technologies, paving the way for sustainable and effective solar power generation systems. Continued research in this field will further refine our ability to harness solar energy for a cleaner and more sustainable future.

### References

1. Note on the properties of silicon / R. Hare // Journal of the Franklin Institute. — 1833. — Vol. 15, No. 6. — P. 362–363. [https://doi.org/10.1016/s0016-0032\(33\)90307-5](https://doi.org/10.1016/s0016-0032(33)90307-5)
2. Space radiation applicability of pure silicon-core optical fibers / J. Xiao, Z. Hengjing, Zh. Hongqi, M. Xiping, J. Qiuyang // Infrared and Laser Engineering. — 2017. — Vol. 46, No. 8. — P. 822002. <https://doi.org/10.3788/irla201746.0822002>
3. The semiconductor silicon industry roadmap: Epochs driven by the dynamics between disruptive technologies and core competencies / S.T. Walsh, R.L. Boylan, C. McDermott, A. Paulson // Technological Forecasting and Social Change. — 2005. — Vol. 72, No. 2. — P. 213–236. [https://doi.org/10.1016/S0040-1625\(03\)00066-0](https://doi.org/10.1016/S0040-1625(03)00066-0)
4. Amorphous silicon enhanced metal-insulator-semiconductor contacts for silicon solar cells / S.L. Zhang, J. Shao, L.S. Hoi, S.N. Wu, B.F. Zhu, F. Shou-Shan, H.D. Li, D.P. Yu // Physica Status Solidi C: Conferences. — 2005. — Vol. 2., No. 8. — P. 3090–3095. <https://doi.org/10.1002/pssc.200460765>
5. Silicon-doped carbon semiconductor from rice husk char / S. Maiti, P. Banerjee, S. Purakayastha, B. Ghosh // Materials Chemistry and Physics. — 2008. — Vol. 109, No. 1. — P. 169–173. <https://doi.org/10.1016/j.matchemphys.2007.11.011>
6. Solid-state physics: Super silicon / R.J. Cava // Nature. — 2006. — Vol. 444, No. 7118. — P. 427–428. <https://doi.org/10.1038/444427a>
7. Carrier heating and its effects on the current-voltage relations of conventional and hot-carrier solar cells: A physical model incorporating energy transfer between carriers, photons, and phonons / C.-Y. Tsai // Solar Energy. — 2019. — Vol. 188. — P. 450–463. <https://doi.org/10.1016/j.solener.2019.06.024>
8. Electrical characteristics and hot carrier effects in quantum well solar cells / D.-T. Nguyen, L. Lombez, F. Gibelli, M. Paire, S. Boyer-Richard, O. Durand, J.-F. Guillemoles // Proceedings of SPIE - The International Society for Optical Engineering. — 2017. — Vol. 10099. — P. 127693. <https://doi.org/10.1117/12.2251331>
9. Direct measurement of the internal electron quasi-fermi level in dye sensitized solar cells using a titanium secondary electrode / K. Lobato, L.M. Peter, U. Würfel // Journal of Physical Chemistry B. — 2006. — Vol. 110, No. 33. — P. 16201–16204. <https://doi.org/10.1021/jp063919z>
10. The open-circuit voltage in microcrystalline silicon solar cells of different degrees of crystallinity / M. Nath, P. Roca i Cabarrocas, E.V. Johnson, A. Abramov, P. Chatterjee // Thin Solid Films. — 2008. — Vol. 516, No. 20. — P. 6974–6978. <https://doi.org/10.1016/j.tsf.2007.12.052>
11. Solar energy conversion with hot electrons from impact ionisation / P. Würfel // Solar Energy Materials and Solar Cells. — 1997. — Vol. 46, No. 1. — P. 43–52. [https://doi.org/10.1016/S0927-0248\(96\)00092-X](https://doi.org/10.1016/S0927-0248(96)00092-X)

### Information about author:

*Ersaiyn Bekbolsynov* – Master Student, Faculty of Physics and Mathematics, Bukhara State University, 11 Mukhammad Iqbol st., Bukhara, Uzbekistan, [ersaiynb@mail.ru](mailto:ersaiynb@mail.ru)

### Author Contribution:

*Ersaiyn Bekbolsynov* – concept, methodology, resources, data collection, testing, modeling, analysis, visualization, interpretation, drafting, editing, funding acquisition.

**Conflict of Interest:** The authors declare no conflict of interest.

**Use of Artificial Intelligence (AI):** The authors declare that AI was not used.

*Received: 09.03.2024*

*Revised: 25.04.2024*

*Accepted: 01.05.2024*

*Published: 03.05.2024*



**Copyright:** © 2024 by the authors. Licensee Technobius, LLP, Astana, Republic of Kazakhstan. This article is an open access article distributed under the terms and conditions of the Creative Commons Attribution (CC BY-NC 4.0) license (<https://creativecommons.org/licenses/by-nc/4.0/>).